

TRANSIENT KINETIC STUDIES OF CHAR REACTIONS
IN A GRADIENTLESS REACTOR SYSTEM -- CO₂ GASIFICATION

O. Sy and J. M. Calo

Division of Engineering
Brown University
Providence, Rhode Island 02912

1. INTRODUCTION

Although a voluminous literature exists concerning the study of coal char-gas reaction systems, the understanding of the actual mechanisms and the roles of heat and mass transport in the overall conversion process, are still far from complete. One difficulty in determining intrinsic reaction mechanisms in many previous studies can be at least partially attributed to the use of "steady-state" conditions. The results of such experiments can be explained equally well by a few plausible models which all yield roughly the same overall gasification rate. Discrimination among candidate models is difficult under these conditions, and there is no guarantee that the model finally selected actually reflects the true mechanism over a wide range of operating conditions. Also, "steady-state" rate measurements reveal relatively little concerning the detailed sequence of elementary steps that constitutes the intrinsic reaction mechanism.

In addition to difficulties in model discrimination, the types of laboratory reactors which have been used in coal gasification kinetic studies may have also contributed to data interpretation problems that are well known for heterogeneous catalytic systems [e.g., see (1-3)].

The primary objective of the current work is to overcome most of these problems in order to develop a fundamental description of the reaction mechanisms of the heterogeneous coal char-gas reactions using an experimental system and techniques which allow the elementary steps to be better identified. More specifically, the approach involves the application of a "gradientless" reactor system coupled with a supersonic, modulated molecular beam mass spectrometer, and transient response techniques to char gasification kinetic studies. The transient behavior of a reaction system as it proceeds from one steady-state to another upon perturbation of system state variables exhibits characteristics reflective of the nature of the detailed kinetic mechanism. Furthermore, in addition to transient data, the usual steady-state results are available as well. Thus the transient response method is employed as an aid in model discrimination, mechanism determination, and, ultimately, parameter estimation.

The use of an internal recycle, "gradientless" reactor serves a dual purpose: (1) it simplifies the mathematical analysis of the transient data due to the resultant lumped parameter description of the transient response; and (2) it significantly reduces the influence of interphase mass and heat transport gradients. The principal advantages of this type of reactor over other common reactor types have been well documented in the literature [e.g., see (3-11)].

Finally, in order to obtain the transient data, the reactor must be coupled to a responsive analytical technique which allows continuous measurement of the transient product concentrations. Mass spectrometry is one such technique compatible with the transient response method. On-line mass spectrometry has been employed by several researchers in studies of the devolatilization of coal under vacuum conditions (12-14). Rapid sampling while operating at the high pressures relevant to the present study can be accomplished by allowing the product gases after pressure let-down to expand through a sonic orifice as a supersonic, adiabatic free jet into a differentially-pumped vacuum system. The rapid expansion into the vacuum "freezes" the relative compositions of the product gases when the sampled gas attains molecular flow. By skimming the core of the jet, a molecular beam can be formed. The resultant beam is further modulated to discriminate between the in-

stantaneous behavior of the beam species and the same species in the background of the mass spectrometer vacuum envelope (15,16).

The adaptation of these techniques to the current purpose is set forth below. The char-carbon dioxide reaction system is used to illustrate the efficacy of the approach. Other char-gas reaction systems and related studies are being pursued in a similar manner.

2. EXPERIMENTAL

2.1. System Description

A schematic of the experimental apparatus developed for the current transient kinetic studies is presented in Figure 1. Essentially, it consists of: (a) a continuous gas flow, fixed solids, "gradientless" (Berty-type) reactor; (b) an automatic switching gas addition valve network for generating concentration perturbations under conditions of constant flowrate, temperature, and pressure; and (c) a supersonic, modulated, molecular beam mass spectrometer for measuring the transient behavior of the concentrations of the product gases.

A typical experimental run might proceed in the following manner. Steady-state is first established with inert gas (e.g., argon) flowing through the reactor (maintained at the desired temperature and pressure), and with reactant gas (e.g., carbon dioxide) flowing through the purge line. At time zero, the inert gas is instantaneously replaced by the reactant gas now flowing through the reactor, and the reaction is thereby initiated. The switching is done in such a manner as to insure the same volumetric flowrate through the reactor, in spite of the change in gas species. This results in a well-defined step function increase of the reactant to the reactor. The transient response of the reaction system to this perturbation is then monitored with the beam sampling system at the reactor exit.

The experimental system has been designed to operate at conditions relevant to commercial coal gasification conditions (e.g., up to 500 psi at 1400°F, and even higher pressures at lower temperatures, as determined primarily by the manufacturer's specifications for the reactor). Also, the reactor space time (the ratio of the reactor gas phase volume to the volumetric flowrate) can be varied over the range 0.01 - 1.0 min.

The preceding, necessarily brief description is intended to convey only a general overview of the apparatus and its mode of operation. For a thorough discussion of the important and interesting details of the development of the apparatus, and the adaptation of transient kinetic techniques to char gasification, see reference (17).

2.2. System Performance

Reactor mixing performance curves were obtained by imposing step changes in the reactor feed from argon to carbon dioxide at constant volumetric flowrate, pressure, and temperature, and recording the resultant transient response. Due to considerable adsorption of test gases by the char, nonporous 3 mm glass beads were used in the basket for these studies. The resultant data were all clearly exponential, in accordance with well-mixed reactor behavior, and the corresponding time constants were close to expected values. The total gas mixing volume deduced from these experiments was found to be 241.4 cm³, which is quite reasonable in view of the fact that the total internal reactor volume is 275 cm³, of which approximately 30 cm³ is presumed to be dead volume located beneath the impeller.

In order to assess the relative influence of interphase heat and mass transfer on intrinsic chemical kinetic rates, the reactor internal recycle ratio, R , and superficial velocity, v_0 , through the char bed were determined by measuring the pressure drop across the char bed in the same manner as described by Berty (18); i.e., $R = A v_0 / q$, where A is the cross-sectional area of the basket (20.27 cm²) and q is the volumetric flowrate at reactor conditions. For typical experimental conditions with space time $\tau = 15$ s, free gas volume $V_g = 220$ cm³ ($V_g = 241.4$ cm³ - W/ρ_s , where W is the weight of dry char in the basket, ρ_s is the solid density and 241.4 cm³ is the total free gas volume in the reactor from the glass beads experiments), and impeller speed of 2800 RPM, the superficial gas velocity deter-

mined from our calibration is $v_o = 13.72$ cm/s (0.45 ft/s). With a flowrate of $q = 14.67$ cm³/s the recirculation ratio is $R = 19$, which is sufficient to guarantee good mixing and gradientless operation.

The influence of interphase mass transfer limitation on measured kinetics for a particular set of experimental conditions can be assessed from the Damkohler number, $Da = k_1 C_{so} (1-\theta) / k_m a_m / RT$, which is the ratio of the reaction rate, (as represented by the kinetic rate constant for the oxygen-exchange reaction; see below), and the effective interphase mass transfer coefficient for CO₂ which can be estimated from the j -factor for interphase mass transfer, j_D (e.g., see (19), p.395). For the experimental conditions used in the current work, it was found that $1 \times 10^{-6} < Da < 9 \times 10^{-4}$. Since $Da \ll 1$, the reaction is definitely not limited by interphase mass transport. The relative importance of intraphase diffusion is considered in the Discussion.

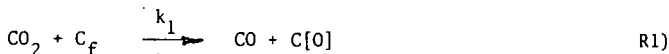
The interphase heat transfer limitation can also be evaluated from the Damkohler number by making use of the Chilton-Colburn analogy between mass and heat transfer in packed beds (e.g., see (19), p. 396). For typical reaction conditions, assuming a heat of reaction of +41.23 kcal/g mol for the overall CO₂ - char gasification reaction, the estimated temperature difference between the surface of the char, T_s , and the bulk fluid, T_b , is $5 \times 10^{-6} < (T_b - T_s) / T_b < 4 \times 10^{-3}$. Thus, for a high operating temperature like 972 K, $(T_b - T_s)$ can be as large as 4°C. Actual temperature differences between the solid and gas in the char bed are expected to be less than this due to radiation. Therefore, it can be conservatively stated that the interphase heat transfer limitation is not significant in the current studies.

Based upon the preceding performance data and numerical estimates, the particle size of the activated coconut (Fischer) char selected for the experiments reported on here was > 14 mesh. With an average particle diameter of about 1.6 mm, the resultant superficial velocity through the char bed at maximum impeller RPM should effectively eliminate interphase heat and mass transfer gradients, and provide a relatively high internal recycle ratio for space times in the range of 12 to 20s, that were found to be optimum for the current experiments.

3. KINETIC MODELING

The general treatment of transient kinetic models is outlined by Bennett (20) and Cutlip et al. (21). In essence, the transient mass balances for the species in the reaction system yield a set of differential equations which defines the model for the particular mechanism assumed. Integration of this system of equations results in the transient curves of the various species, which can then be used for parameter sensitivity studies, and also for parameter estimation by comparison with corresponding experimental data.

In order to illustrate this approach, consider the simple two-step mechanism:



which is imbedded in all known CO₂ gasification kinetic mechanisms, and was found to adequately represent the data in the current work.

If C_{so} , C_o , x , θ , and P_i represent, respectively, the active site concentration in g mol/g mol C, the initial total g mol of carbon, the fractional conversion, the fractional surface coverage of the complex, and the partial pressure of species i in the gas phase, the following rate expressions result for the preceding mechanism:

$$r_1 = C_{so} C_o (1-x) [k_1 (1-\theta) P_{CO_2}] \quad 1)$$

$$r_2 = C_{so} C_o (1-x) [k_2 \theta] \quad 2)$$

Assuming a gradientless reactor, a mass balance on each species yields:

$$CO_2: \quad \frac{dP_{CO_2}}{dt} = \frac{P_{CO_2}^0 (1-\delta) - P_{CO_2}}{\tau} - \frac{r_1 RT}{V_g} \quad 3)$$

$$CO_2: \quad \frac{dP_{CO}}{dt} = \frac{(r_1 + r_2)}{V_g} - \frac{P_{CO}}{\tau} \quad 4)$$

$$C[O]: \quad \frac{d\theta}{dt} = \frac{r_1 \frac{g}{C_{SO}} r_2}{C_{SO} C_O (1-x)} + \frac{\theta r_2}{C_O (1-x)} \quad 5)$$

$$C: \quad \frac{dx}{dt} = \frac{r_2}{C_O} \quad 6)$$

$$\text{Inert gas (Ar): } P_{Ar} = P_{CO_{2f}} - P_{CO_2} - P_{CO} \quad 7)$$

where $\delta = \frac{r_2 RT \tau}{V_g P_{CO_{2f}}}$ (due to the increase in gas volume upon reaction)

P_t = total system pressure, atm

$P_{CO_{2f}}$ = partial pressure of CO_2 in the feed (also total pressure of reactor if feed is pure CO_2), atm

τ = V_g/q ; reactor space time evaluated at reactor conditions, min

V_g = reactor gas phase volume, cm^3

q = volumetric flowrate at reactor conditions, cm^3/min

T = reaction temperature, K

R = universal gas constant, $atm \cdot cm^3 / K \cdot g \text{ mol}$

The units for the rate parameters are $k_1 = [min^{-1} atm^{-1}]$ and $k_2 = [min^{-1}]$. The initial conditions for a pure CO_2 feed at time $t = 0$ are:

$$\begin{aligned} P_{CO_2} &= P_{CO} = \theta = x = 0 \\ P_{Ar} &= P_t \end{aligned} \quad 8)$$

Equations 1 through 8 constitute the model for the reaction system with dependent variables P_{CO_2} , C_{CO} , P_{Ar} , θ , and x , and parameters C_{SO} , k_1 , and k_2 .

From simulated CO transient response results, it was found that the active site concentration, C_{SO} , has a pronounced effect on the production of CO, but the shape of the transient curve remains relatively unchanged. However, the shape and position in time of the "overshoot" of the CO responses for both mechanisms are quite sensitive to the kinetic rate parameters k_1 and k_2 . The effects of k_1 and k_2 are qualitatively illustrated in Figure 2. It is noted that the "overshoot" is due to large values of k_1 , while the "leveling-off" is associated with large k_2 values.

Once the raw data (i.e., transient curves of the modulated signals for $m/e = 44$ and 28) are corrected to yield the net CO production curve due to reaction (from the fragmentation coefficient measured for CO_2), and then converted to CO partial pressure data (from the relative sensitivity measured for CO and CO_2), the next step is to determine a best parameter set for the proposed mechanism. This is done by minimizing the least squares objective function,

$$\phi = \sum_{k=1}^{\xi} \sum_{i=1}^{\eta} [(\hat{y}_{ik} - \hat{y}_{ik})/y_{ik}]^2 \quad 9)$$

(where the subscript ik represents the ith variable at time k, with:

$i = 1, \dots, n$; the number of variables used in the optimization process,

$k = 1, \dots, ;$ the time intervals

y_{ik} = experimental point (partial pressure data),

\hat{y}_{ik} = predicted value from the model,

using a Marquardt-type technique (22), coupled with a Green's function method (23) to determine the necessary first order sensitivity coefficient matrix, $S = \partial y / \partial \beta$. In essence, the parameter estimation procedure consists of solving the $\sim \sim \sim$ equations resulting from minimizing the objective function, Equation 9, based on local linearization of the model about the initial guess parameter set, β . This solution yields the vector of parameter changes, Δb_i , which in turn gives $\sim \sim$ the next best estimate of the parameter set to minimize ϕ . This procedure is repeated until the objective function meets an acceptable preset tolerance. In the current work only one variable, P_{CO} , was used in the optimization of the objective function for parameter estimation from the experimental transient data. This was done because this variable is the most sensitive to the particular model used, while P_{CO_2} and P_{Ar} are less so.

4. RESULTS

The CO transient responses for the experimental runs conducted with two particle sizes of activated coconut (Fischer) char are presented in Figures 3 and 4. In these figures, the characteristic "overshoot" of the oxygen-exchange reaction, R1, as well as the "leveling-off" of the transient curves due to the carbon gasification reaction, R2, are clearly evident. As predicted by transient response simulations, smaller space times result in a sharper "overshoot" and a lower quasi-steady-state level of CO at longer times. Higher temperatures favor greater CO production but the "overshoot" becomes progressively less sharp.

The inhibition effect of pressure on gasification is not clearly evident in these figures, but becomes more so upon analysis of the quasi-steady-state gasification rate attained after "leveling-off" of the transient curves. From the stoichiometry of the overall reaction:



For continuous pure CO₂ gas feed, the "steady-state" gasification rate is given by

$$W_{ss} = \frac{-1}{dC} \frac{dC}{dt} = \frac{1}{2C} \frac{d[CO]}{dt} = \frac{P_{CO_{ss}}}{2C_o(1-x)RT} \approx \frac{P_{CO_{ss}}}{2C_o RT} \quad (10)$$

for negligibly small carbon conversion (i.e., $x \approx 0$).

Equation 10 can be rearranged to

$$\left(\frac{P_{CO_2}}{W} \right)_{ss} = \left(\frac{2C_o RT}{q} \right) \left(\frac{P_{CO_2}}{P_{CO}} \right)_{ss} \quad (11)$$

The $(P_{CO_2}/P_{CO})_{ss}$ in this expression can be evaluated from the quasi-steady-state values \sim obtained at the end of the transient period. A plot of the right-hand side of Equation 11 versus P_{CO_2} at constant temperature is presented in Figure 5. The observed linear dependence \sim of the gasification rate on CO₂ partial pressure suggests a "steady-state" rate expression of the form:

$$\frac{P_{CO_2}}{W_{ss}} = \frac{1}{j_1} + \frac{P_{CO_2}}{j_2} \quad (12)$$

or

$$W_{ss} = \frac{j_1 P_{CO_2}}{1 + (j_1/j_2) P_{CO_2}} \quad (13)$$

Equation 13 is the same steady-state rate form observed by Ergun (24), with $j_1 = k_1 C_{S_o}$ and $j_2 = k_2 C_{S_o}$, and clearly shows the inhibiting effect of pressure on the gasification rate.

Several models were fit to the transient data: the Blackwood and Ingeme model (25), seven parameters; the Shaw model (26), five parameters; the Mentser and Ergun mechanism (27), five parameters; the Ergun mechanism (24), four parameters; and the two-step mechanism found appropriate in the current work (three parameters). Due to the low levels of CO present in the reactor under the current experimental

conditions, only the latter model fits the data accurately since the others all have CO reaction paths which are superfluous for our data.

The resultant parameter values for the two-step mechanism exhibited distinct Arrhenius temperature dependence. Numerical fits of all the data as a function of temperature yielded the following expressions:

$$k_1 = 6.13 \times 10^{11} \exp \left[\frac{-55,500}{RT} \right] \quad \text{min}^{-1} \text{atm}^{-1} \quad (14)$$

$$\text{and } k_2 = 9.98 \times 10^9 \exp \left[\frac{-44,800}{RT} \right] \quad \text{min}^{-1} \quad (15)$$

Also, for the first time in the same experiment, the concentration of active carbon sites expressed as g mol/g mol C, was determined for the coconut char to be:

$$C_{SO} = 1.70 \times 10^{-9} \exp \left[\frac{27,000}{RT} \right] \quad (16)$$

This indicates that the active site concentration has a negative "activation energy". In other words, at higher temperatures, initially active sites become deactivated; viz.,



This deactivation phenomenon agrees with some of the findings of Duval (28) and Blackwood et al. (29), which are discussed further below.

It is of interest to compare the values of the activation energies obtained in the present study for the two steps, R1 and R2, with corresponding values reported in the literature. Table I summarizes the results of previous investigators. It is evident that the apparent activation energy for the two common kinetic steps varies considerably from one study to another; with E_1' ranging from -27 to +76 kcal/g mol and E_2' from -17 to +93 kcal/g mol. This variation can be at least partially attributed to differences in experimental data analysis techniques, as well as the particular reaction mechanism assumed. It should also be noted that in all these studies, the rate parameters are reported as the product of the active site concentration, C_{SO} , and the intrinsic rate constant, k . Hence, the apparent activation energies also reflect any variation of C_{SO} with temperature. In other words, the difference in the types of char and experimental conditions can account for the wide range of activation energies evident in Table I. As indicated by Johnson (30), C_{SO} is expected to decrease with increasing coal rank. In fact, this general trend is substantiated in the case of $k_2 C_{SO}$ by the large activation energies observed for the high purity carbon (e.g., Ceylon graphite, Spheron 6 carbon, activated carbon, and graphite) used by Ergun (24) and Mentser and Ergun (27), vis-a-vis the much smaller temperature coefficients found for coconut char by Gadsby et al. (31), Long and Sykes (32), and also in the current work.

Differences in activation energies can also be attributed to presumably catalytic impurities in the char. This effect is especially pronounced (for $k_2 C_{SO}$) in the work of Long and Sykes (32) with coconut char where E_2' changed from 38 to 66 kcal/g mol upon removal of mineral impurities with hydrochloric and hydrofluoric acids.

On the other hand, Mentser and Ergun (27) argued that the constant activation energies obtained in their work with different forms of high purity carbon were due to a constant number of active sites, C_{SQ} , independent of temperature, and thus reflected the true activation energies for the reaction steps. This hypothesis is not at all unreasonable since C_{SO} should not decrease indefinitely with coal rank, but rather the active site concentration should attain some constant asymptotic value for the high purity carbons. If the activation energies reported by Mentser and Ergun are the "true" temperature coefficients for R1 and R2 (with $E_1 = 53.0$ kcal/g mol and $E_2 = 58.0$ kcal/g mol), then their results agree reasonably well with the intrinsic activation energies found in the current work ($E_1 = 55.5$ kcal/g mol and $E_2 = 44.8$ kcal/g mol).

Other differences in E_1' and E_2' are probably numerical in origin. For instance, Golovina (33) fitted several simplified forms of the same gasification rate expression to data (i.e., due to possible changes in mechanism at various conditions), and reported different E' values for three different regimes of pressure and temperature. However, the negative activation energies obtained are indicative of improper analysis of kinetic data. In addition, the fact that the same rate form can give rise to different apparent activation energies in different temperature regimes but over the same pressure range (see Table I, as reported by Golovina, also argues against the inherent validity of the proposed rate expression and the reaction rate - controlling zone claimed by the investigator.

The effect of intraphase mass transport resistance on the rate constants is now addressed. First, there was no discernible difference in the gasification rate behavior of the 1.6 mm and 2.68 mm coconut char particles. Also, the resultant model parameters for the two-step mechanism exhibit essentially the same temperature dependence for both particle sizes. However, chars generally exhibit a polymodal pore size distribution with most of the internal surface area available in pores of molecular dimensions (super micropores) (34). Thus, even though the insensitivity to particle size indicates no bulk diffusional limitation (i.e., in the macropores), if diffusion in the micropores were the limiting resistance to char gasification, particle size would not necessarily have any effect; i.e., the characteristic size of the microporous material in both particle sizes is similar. In addition, micropore diffusion is known to be activated (35). Thus if its rate is comparable to the kinetic rate, or rate-controlling, its activation energy would be included in the overall apparent activation energy.

The diffusion parameter (diffusion time constant) of CO_2 in the micropores of WYODAK 35 x 60 char at 800°C is given by Debelak and Malito (36) as $D/r^2 = 1.68 \text{ min}^{-1}$ for fresh char (i.e., $x = 0$). The coconut char gasification rate at 800°C and 1 atm in pure CO_2 , as given by Equation 13 with the rate parameters reported here, is $1.16 \times 10^{-3} \text{ min}^{-1}$. Thus, if the microporous structure of the WYODAK and coconut chars are at all similar, the observed gasification rate is too small by three orders-of-magnitude to be micropore diffusion-controlled. Even at the highest possible constant asymptotic gasification rate (i.e., at high pressure) of $4.02 \times 10^{-3} \text{ min}^{-1}$ at 800°C, the reaction is still definitely reaction rate-controlled.

Based on these observations, it is concluded that the activation energies for the parameters k_1 and k_2 found in the present study are intrinsic and in agreement with the general trend reported in the literature.

The negative "activation energy" exhibited by the active site concentration is consistent with the results of Duval (28), who presented strong evidence that active sites on a graphitic lattice disappear spontaneously with reaction temperature by a process termed thermal "healing" or "annealing". Thus, in effect, active sites are subjected to two modes of depletion: reaction with a gas phase molecule and thermal neutralization. Boulangier (37) also noted the same effect in carbon - CO_2 and carbon-steam systems. A similar trend was reported by Blackwood et al. (29) and Johnson (30) in studies of the effects of coal-char preparation temperatures. Blackwood et al. (29) correlated their results for hydrogen gasification rate constants in terms of $k = k^* \exp(E_p/RT_p) \exp(-E_g/RT_g)$, where T_g and T_p are the gasification and char preparation temperatures, respectively. For brown coal chars gasified in hydrogen at 25 atm with $T_p = T_g$, these workers found $E_p = 20 \text{ kcal/g mol}$. It is noted that there is a direct analogy between $T_p = T_g$ in these char reactivity studies and conditions in the current work whereby the coconut char was held at the reaction temperature in an argon atmosphere for relatively long periods of time prior to imposing the concentration step change to reactant CO_2 . Thus, the temperature dependence of C_{s0} found by Blackwood et al. (29) agrees well with that found by Duval (28) and in the present study. Blackwood et al. (29) proposed that the decreasing reactivity with increasing temperature is due to rearrangement of the carbon structure into a more stable ring

lattice, thereby reducing the availability of free π electrons for the formation of complexes at edges, and stabilizing previously unstabilized bonds.

6. CONCLUDING REMARKS

The efficacy of applying the experimental apparatus and transient response techniques to heterogeneous char-gas reactions has been successfully demonstrated for CO₂ gasification. This approach promises to be a valuable tool for determining mechanisms and rate parameters for direct use in modeling, design, and analysis of new or existing gasification and related systems. A similar approach is being taken in studying gasification reactions with other gases and mixtures.

ACKNOWLEDGEMENT

The authors gratefully acknowledge the support of the U. S. Department of Energy under Grant Nos. DE-FG22-80PC30211 and DE-FG22-81PC40786. However, any opinions, findings, conclusions, or recommendations expressed herein are those of the authors and do not necessarily reflect the views of DOE.

REFERENCES

- (1) Carberry, J. J., *Ind. Eng. Chem.* **56**, 39 (1964).
- (2) Bennett, C. O., Cutlip, M. B., and Yang, C. C., *Chem. Eng. Sci.* **27**, 2255 (1972).
- (3) Mahoney, J. A., *J. Catal.* **32**, 247 (1974).
- (4) Kobayashi, H., and Kobayashi, M., *Catal. Rev.-Sci. Eng.* **10**, 138 (1974).
- (5) Bennett, C. O., *Ibid.* **13**, 121 (1976).
- (6) Yang, C. C., Cutlip, M. B., and Bennett, C. O., in *Catalysis*, Hightower, J. W., Ed., vol. 1, *Proceedings of the Fifth International Symposium Congress on Catalysis*, p. 14-279, Miami, Fla. (1972).
- (7) Berty, J. M., Preprint No. 41F, 70th Annual Meeting of AIChE, New York, N. Y., Nov. 13-17, 1977.
- (8) Tajbl, D. G., Simons, J. B., and Carberry, J. J., *Ind. Eng. Chem. Fund.* **5**, 171 (1966).
- (9) Paspek, S. C., Varma, A., and Carberry, J. J., *Chem. Eng. Edn.* **14**, 78 (1980).
- (10) Halladay, J. B., and Mrazek, R. V., *J. Catal.* **28**, 221 (1973).
- (11) Brown, C. E., and Bennett, C. O., *AIChE J.* **16**, 817 (1970).
- (12) Joy, W. K., Ladner, W. R., and Pritchard, E., *Fuel* **49**, 26 (1970).
- (13) Juntgen, H., and van Heek, K. H., *Ibid.* **47**, 102 (1968).
- (14) Meyer, R. T., and Lynch, A. W., *High Temp. Sci.* **4**, 283 (1972).
- (15) Fenn, J. B., and Anderson, J. B., *Fourth International Symposium on Rarefied Gas Dynamics*, Section 8, p. 311, Toronto (1964).
- (16) Calo, J. M., and Bailey, A. D., *Rev. Sci. Instrum.* **45**, 1325 (1974).
- (17) Sy, O., "Transient Kinetic Studies of Char-Gas Reactions in a Gradientless Reactor: CO₂ Gasification," Masters Dissertation, Princeton University, May 1982.
- (18) Berty, J. M., *Chem. Eng. Progr.* **70**, 78 (1974).
- (19) Smith, J. M., *Chemical Engineering Kinetics*, McGraw Hill, N. Y. (1981).
- (20) Bennett, C. O., *AIChE J.* **13**, 890 (1967).
- (21) Cutlip, M. B., Yang, C. C., and Bennett, C. O., *Ibid.* **18**, 1073 (1972).
- (22) Marquardt, D. W., *J. Soc. Ind. Appl. Math.* **11**, 431 (1963).
- (23) Kramér, M. A., J. M. Calo, and H. Rabitz, *Appl. Math. Model.* **5**, 432 (1981).
- (24) Ergun, S., *J. Phys. Chem.* **60**, 480 (1956).
- (25) Blackwood, J. D., and Ingeme, A. J., *Aust. J. Chem.* **13**, 134 (1960).
- (26) Shaw, J. T., *Fuel* **56**, 134 (1977).
- (27) Mentser, M., and Ergun, S., *U. S. Bur. Mines Bull.* **644** (1973).
- (28) Duval, X., *J. Chim. Phys.* **47**, 339 (1950).
- (29) Blackwood, J. D., McCarthy, D. J., and Cullis, B. D., *Aust. J. Chem.* **20**, 1561, 2525 (1967).
- (30) Johnson, J. L., *Kinetics of Coal Gasification*, Wiley, N. Y. (1979).
- (31) Gadsby, J., Long, F. J., Sleightholm, P., and Sykes, K. W., *Ibid.* **A193**, 357 (1948).
- (32) Long, F. J., and Sykes, K. W., *J. Chim. Phys.* **47**, 362 (1950).

- (33) Golovina, E. S., Carbon 18, 197 (1980).
- (34) Gan, H., Nandi, S. P., and Walker, P. L., Jr., Fuel 51, 272 (1972).
- (35) Walker, P. L., Jr., Fuel 59, 809 (1980).
- (36) Debelak, K. and Malito, J. T., "Effective Diffusivity in Coals as a Function of Conversion," presented at the 56th Colloid and Surface Science Symposium, Blacksburg, VA, June, 1982.
- (37) Boulangier, F., Duval, X., and Letort, M., Proceedings of the Third Conference on Carbon, p. 257, Pergamon Press, N. Y. (1959).

TABLE I.
Comparison of Kinetic Parameters from Different Investigators

Reference	Carbon Type	T(°C)	P(atm)	$k_1 C_{CO} + A_1 \exp(-E_1/RT)$		$k_2 C_{SO} + A_2 \exp(-E_2/RT)$	
				A_1 (min ⁻¹ atm ⁻¹)	E_1 (kcal/gmol)	A_2 (min ⁻¹)	E_2 (kcal/gmol)
1. (31)	coconut char	700-850	0.01 - 1	7.6×10^9	58.8	2.4×10^3	28.7
2. (32)	coconut char	700-800	0.07 - 0.2	7.6×10^9	58.8	3.6×10^3	38.0
	with impurities extracted			3.8×10^{10}	68.4	2.3×10^8	66.0
3. (24)	activated carbon	(a) 700-1000	1	-	-	8.5×10^8	59.0
	activated carbon	(b) 900-1150	1	-	-	8.28×10^7	59.0
	ceylon graphite	(c) 1000-1400	1	-	-	1.55×10^7	59.0
4. (29)	coconut char	790-870	2-40	2.7×10^{11}	76.0	1.13×10^{12}	76.0
5. (27)	Spheron 6	750-850	1	1.54×10^6	53.0	5.15×10^7	58.0
6. (30)	high volatile bituminous coal char (Pittsburgh seam)	870-980	1-35	3.56×10^3	28.4	3.42×10^{10}	65.0
7. (33)	graphite	1380-1530	1	4.7×10^8	75.0	-	-
	"	"	3-10	4.7×10^8	75.0	23.5	18.0
	"	"	2-40	4.7×10^8	75.0	1.9×10^6	56.5
	"	1730-1927	1	3.8×10^{-4}	-27.0	-	-
	"	"	3-10	3.8×10^{-4}	-27.0	67.2	24.5
	"	"	20-40	3.8×10^{-4}	-27.0	0.17	-3.0
	"	2030-2330	1	9.5×10^2	40.0	-	-
	"	"	3-10	9.5×10^2	40.0	7.1×10^{-3}	-17.0
	"	"	20-40	9.5×10^2	40.0	3.0	12.5
8. (38) summary of various chars							
						32.5 to 61.7	-
9. Present Work	activated coconut char	680-770	8-30	1.0×10^3	28.5	17.0	17.9

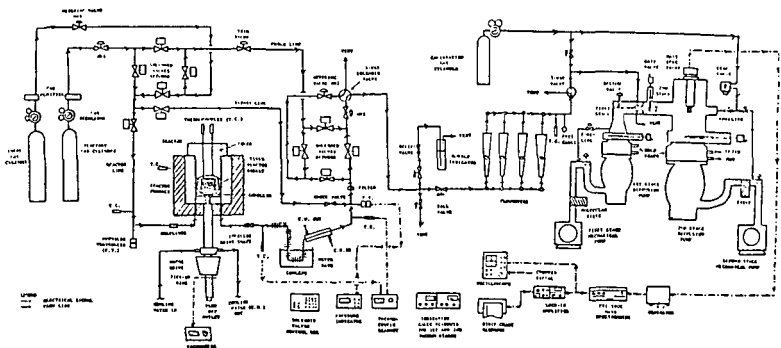


Figure 1. Schematic of the experimental apparatus for transient kinetic studies.

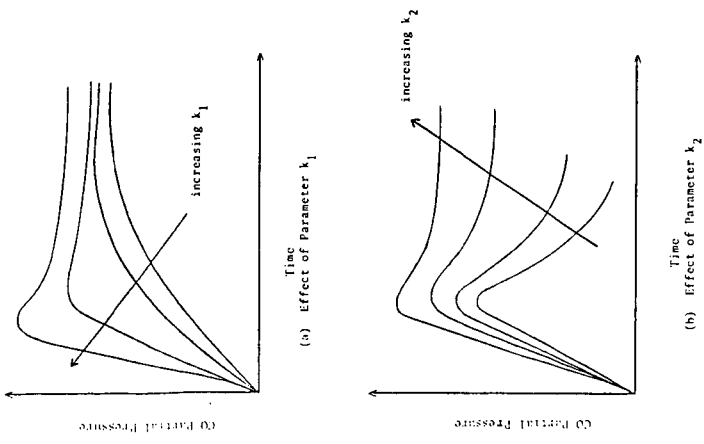


Figure 2. Sensitivity of CO transient response to parameters k_1 and k_2 - qualitative behavior.

Figure 3. Experimental transient response of CO partial pressure versus model predictions for CO₂ gasification of activated coconut char using the two-step mechanism (1.6 mm, 36.1925g, 4.5 cm bed height).

- 16.0 atm, 952 K, $\tau = 0.147$ min, 38.1522g
- 15.8 atm, 986.5 K, $\tau = 0.172$ min, 38.1522g
- △ 16.0 atm, 1001 K, $\tau = 0.198$ min
- 16.3 atm, 1002 K, $\tau = 0.202$ min
- κ 16.2 atm, 1014.5 K, $\tau = 0.192$ min
- ∇ 15.8 atm, 1013 K, $\tau = 0.198$ min
- ◊ 15.9 atm, 1032 K, $\tau = 0.199$ min
- ▲ 15.9 atm, 1033 K, $\tau = 0.214$ min

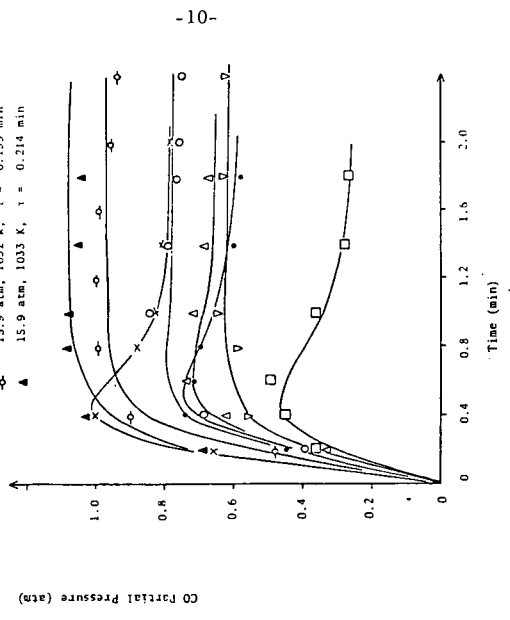


Figure 3. Typical transient response of CO partial pressure for 0.1 mole-% production for CO₂ purification of activated carbon char using the two-step mechanism (2.08 mm, 39.050g, 4.5 cm bed height).

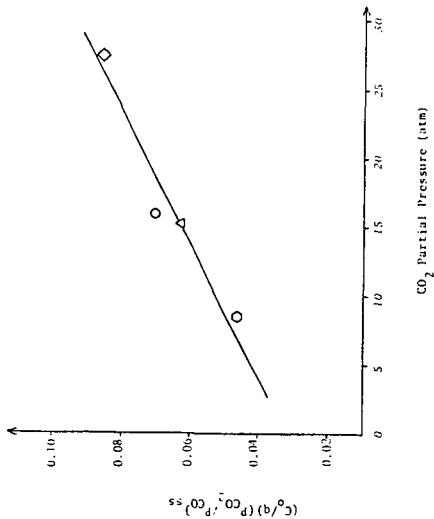
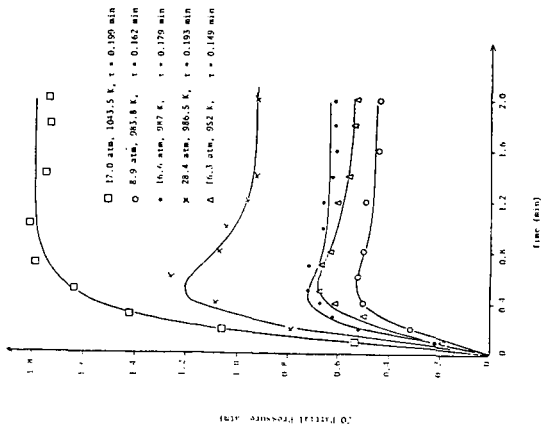


Figure 5. Quasi-steady-state gasification rate as a function of CO₂ partial pressure. (a) 1.6 mm activated carbon char, $P = 16.6$ atm, $\tau = 0.18$ min; (b) 1.6 mm activated carbon char, $P = 15.8$ atm, $\tau = 0.17$ min.